

---

## V.G.1 Fuel Cell Systems Analysis

Rajesh K. Ahluwalia (Primary Contact),  
Xiaohua Wang, Romesh Kumar  
Argonne National Laboratory  
9700 South Cass Avenue  
Argonne, IL 60439  
Phone: (630) 252-5979; Fax: (630) 252-5287  
E-mail: walia@anl.gov

DOE Technology Development Manager:  
Nancy Garland  
Phone: (202) 586-5673; Fax: (202) 586-9811  
E-mail: Nancy.Garland@ee.doe.gov

Start Date: October 2003  
Projected End Date: Project continuation and  
direction determined annually by DOE

### Objectives

- Develop a validated model for automotive fuel cell systems and periodically update it to assess the status of technology.
- Conduct studies to improve performance and packaging, to reduce cost, and to identify key R&D issues.
- Compare and assess alternative configurations and systems for transportation and stationary applications.
- Support DOE/FreedomCAR automotive fuel cell development efforts.

### Technical Barriers

This project addresses the following technical barriers from the Fuel Cells section (3.4.4.2) of the Hydrogen, Fuel Cells and Infrastructure Technologies Program Multi-Year Research, Development and Demonstration Plan:

- (A) Durability
- (D) Thermal, Air and Water Management
- (E) Compressors/Expanders
- (F) Fuel Cell Power System Integration
- (J) Startup Time/Transient Operation

### Technical Targets

This project is conducting system level analysis to address the following DOE 2010 technical targets for the automotive fuel cell power systems operating directly on hydrogen:

- Energy efficiency: 50%-60% (55%-65% for the stack) at 100%-25% of rated power
- Power density: 650 W/L for system, 2,000 W/L for the stack
- Specific power: 650 W/kg for system, 2,000 W/kg for the stack
- Transient response: 1 s from 10% to 90% of rated power
- Start-up time: 30 s from -20°C and 15 s from +20°C ambient temperature
- Precious metal loading: 0.3 g/kW

### Accomplishments

- Developed a model for self-start of polymer electrolyte fuel cell (PEFC) stacks from sub-freezing temperatures using laboratory data obtained under isothermal conditions.
- Initiated work on the effects of fuel impurities and air contaminants on the performance of PEFC stacks.
- Updated Argonne's model for performance of pressurized automotive fuel cell systems by incorporating recent results on stack behavior, anode subsystem, on-board heat rejection, and water management.
- Validated the stack model using performance data from a commercial stack benchmarked at ANL's Fuel Cell Test Facility.
- Validated models for the enthalpy wheel humidifier and the membrane humidifier with experimental data taken at Emprise and Perma Pure, respectively.
- Calibrated the heat rejection models with analytical results from Honeywell for different radiator configurations.

---

### Introduction

While different developers are addressing improvements in individual components and subsystems in automotive fuel cell propulsion systems (i.e., cells, stacks, fuel processors, balance-of-plant components), we are using modeling and analysis to address issues of thermal and water management, design-point and part-load operation, and component-, system-, and vehicle-level efficiencies and fuel economies. Such analyses are essential for effective system integration.

## Approach

Two sets of models are being developed. The software GCTool is a stand-alone code with capabilities for design, off-design, steady-state, transient and constrained optimization analyses of fuel cell (FC) systems. A companion code, GCTool-ENG, has an alternative set of models with a built-in procedure for translation to the MATLAB/SIMULINK platform commonly used in vehicle simulation codes such as PSAT.

## Results

In FY 2005, we formulated a detailed two-dimensional model to analyze the electric field, current distribution, species concentration, and formation and melting of ice within a representative cell. In FY 2006, we used results from the 2-D formulation to write a simpler model that is suitable for conducting parametric analyses to determine the conditions under which PEFC stacks can be self-started from sub-freezing temperatures. The simple model was validated against experimental data for startup behavior of a single cell from  $-10^{\circ}\text{C}$  to  $-25^{\circ}\text{C}$  at 1 to 2 bar [1]. The experiments were conducted under isothermal conditions by positioning the cell inside an environmental control chamber. Figure 1 compares the calculated and measured voltage decay profiles at  $-20^{\circ}\text{C}$  with dry feeds. In agreement with the data, the model shows that there is a critical current density, at which the cell can be operated stably, but above which the cell voltage declines with time. The decline is gradual initially, but becomes more rapid once the volume fraction of ice in the cathode catalyst layer exceeds 0.8–0.9. The cell voltage declines faster if the cell is operated at higher current density, elevated pressure, or lower temperature.

The model was used to analyze the startup behavior of a pressurized automotive PEFC stack (820 W/kg specific power with graphite bipolar plates, 2.5 bar at

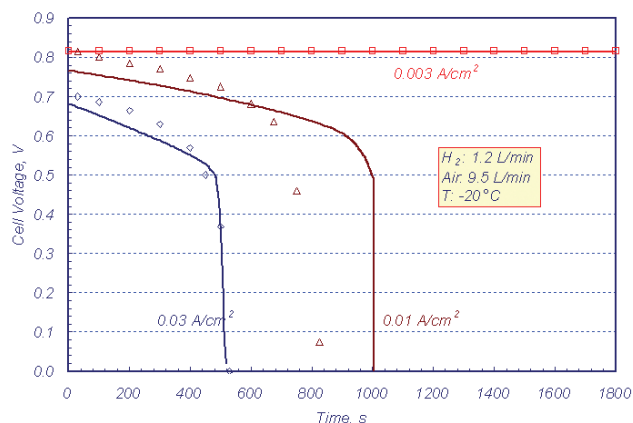


FIGURE 1. Isothermal Voltage Decay Profile at  $-20^{\circ}\text{C}$

rated power) under non-isothermal conditions. Figure 2 presents results from one set of simulations in which the stack is initially free of ice at  $-20^{\circ}\text{C}$ , the ambient temperature is also  $-20^{\circ}\text{C}$ , and the air and hydrogen flows are at 50% of rated capacity. Figure 2a shows the existence of a critical cell voltage ( $V_c$ ), above which self-start is not possible. The critical voltage ( $\sim 0.5$  V at  $-20^{\circ}\text{C}$ ) is a function of the initial stack temperature; the lower the initial stack temperature, the lower the critical voltage. For  $V > V_c$ , the average current density decreases with time (see the curve for 0.7 V) because of the buildup of ice in the cathode catalyst layer. For  $V = V_c$  (see the curve for 0.5 V), the current density initially increases with time as the stack heats up, but there is an intermediate period of time (75–100 s), during which the current density decreases with time because of diminishing effective electrochemical surface area (ECSA). At 100 s, the ice begins to melt, leading to the recovery of ECSA and the current density then climbs sharply. For  $V < V_c$  (see the curve for 0.3 V), the startup is faster and more robust, in that the current density increases monotonically with time. The startup is even faster if the cell is operated closer to the short circuit condition, e.g., at 0.1 V rather than at 0.3 V.

Figure 2b tracks the buildup and disappearance of ice in the cathode catalyst layer. For  $V > V_c$ , ice volume fraction increases gradually. Ice builds up faster if the stack is operated at  $V < V_c$ ; however, ice volume fraction reaches a peak value and then decreases precipitously as the stack reaches  $0^{\circ}\text{C}$ . Below  $V_c$ , the lower the cell voltage, the smaller the peak value of ice volume fraction. For  $V > V_c$ , the stack is heated slowly and equilibrates at a temperature below the melting point of ice. This is why the stack cannot be self-started from subfreezing temperatures at  $V > V_c$ . The stack is heated faster and to temperatures above  $0^{\circ}\text{C}$  if  $V < V_c$ . Also, the lower the cell voltage, the faster the rise in stack temperature.

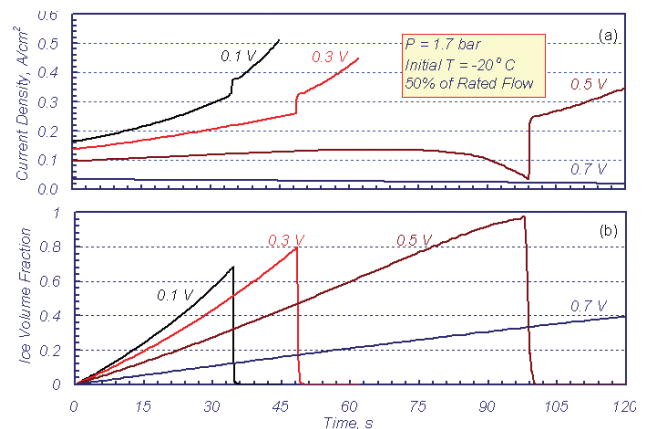


FIGURE 2. Effect of Cell Voltage on Startup from  $-20^{\circ}\text{C}$ : a) Current Density, b) Ice Coverage in Cathode Catalyst Layer

There are three reasons why the startup from subfreezing temperatures is faster at near short circuit conditions. First, hydrogen utilization is proportional to the amount of current that can be passed. The higher the current, the larger the amount of hydrogen consumed in the electrochemical reaction and the faster the rate at which the stack warms up. Second, the higher the current density, the lower the cell voltage and more waste heat is generated. At short circuit, the stack does not produce any electrical power; instead all of the energy of the cell reaction is converted into waste heat that is absorbed by the stack. Third, a fraction of the water that is produced at the cathode is transported into the gas diffusion layer (GDL). The higher the current density, the larger the fraction of water that is transported to GDL. By operating at a high current density, a larger fraction of ice forms in the GDL rather than in the cathode catalyst layer. This provides additional time to allow the cell temperature to rise above 0°C before the ice can completely cover the cathode catalyst and shut down the electrochemical reaction.

### Behavior of Nitrogen in the Fuel Cell Stack

Over the past year, we have considered the issue of nitrogen diffusion across the fuel cell membrane, the effect of this crossover on fuel cell performance, need for anode gas purging, etc. This analysis is for a fuel cell system with anode gas recycle, along with a controlled purge of the recycled gas to control the build up of  $N_2$  in the anode gas. An increasing purge fraction reduces the maximum concentration of  $N_2$  in the anode gas, thereby limiting the decrease in cell voltage due to dilution of the  $H_2$ ; however, the increasing purge rate makes increasing amounts of  $H_2$  unavailable for electrochemical oxidation. Several other parameters also enter into the analysis, but an optimum purge rate may be determined such that the overall decrease in system efficiency, compared to a system with no  $N_2$  crossover, is minimized. Of course, anode gas purging may also be driven by factors other than the buildup of inert gases, but such factors were not considered in the present analyses.

For these analyses, we defined a reference fuel cell system (FCS) with 50% efficiency (LHV) at rated power. Design and operating parameters include pure  $H_2$  feed from the fuel tank; 90% or 70%  $H_2$  utilization per pass (i.e., 1.1 or 1.4 stoichs, respectively); 25- and 50- $\mu\text{m}$ -thick membranes, 200- $\mu\text{m}$ -thick GDL; and recycle of 100% of the  $H_2$  in the spent anode gas. A correlation for the  $N_2$  permeance was developed using data reported by Mittelsteadt and Umbrell [2]. Gas crossovers ( $N_2$ ,  $H_2$ ,  $O_2$ ) were modeled as functions of current density, relative humidity, temperature, and membrane thickness.

With pure  $H_2$  fuel, at 10% of rated power, 90% fuel utilization per pass, and a low purge rate,  $N_2$  can buildup to 25% to 50% (anode inlet and outlet, respectively),

and even with a relatively high 2% purge rate, it can buildup to 5% to 25% (anode inlet/outlet). The effect of this amount of nitrogen on cell voltage is shown in Figure 3. With a relatively high 2% purge rate, the cell voltage decreases by <5 mV; at a low purge rate of 0.1%, the cell voltage can decrease by ~20 mV (due to  $N_2$  concentration reaching 25–50% levels).

Under optimum purge conditions,  $N_2$  concentrations at the stack outlet are similar with 70% and 90% fuel utilizations and different levels of  $N_2$  impurity in the fuel  $H_2$ , as shown in Figure 4. The net effect of  $N_2$  buildup for a 25- $\mu\text{m}$ -thick membrane and 70% fuel utilization per pass is to decrease the stack efficiency by 0.1-1 percentage points for 0.1-1.5%  $N_2$  in fuel  $H_2$ .

### Performance of Automotive Fuel Cell Systems

In support of the TIAX cost study, we updated the performance of the automotive FCS by incorporating recent results on catalyst loading, crossover of gases, heat rejection, and water management. We considered

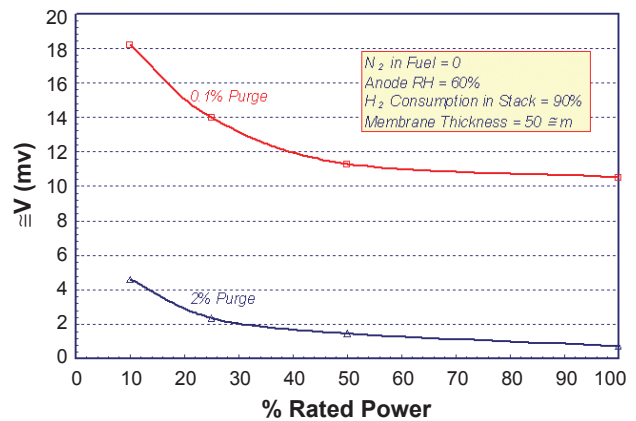


FIGURE 3. Effect of Nitrogen Buildup on Cell Voltage

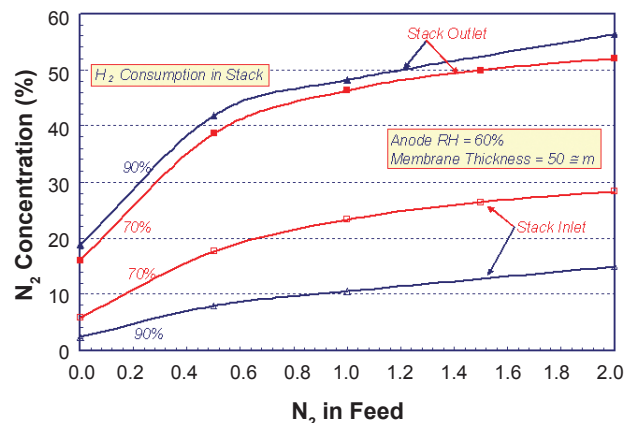


FIGURE 4. Effect of Fuel Utilization on Nitrogen Concentration

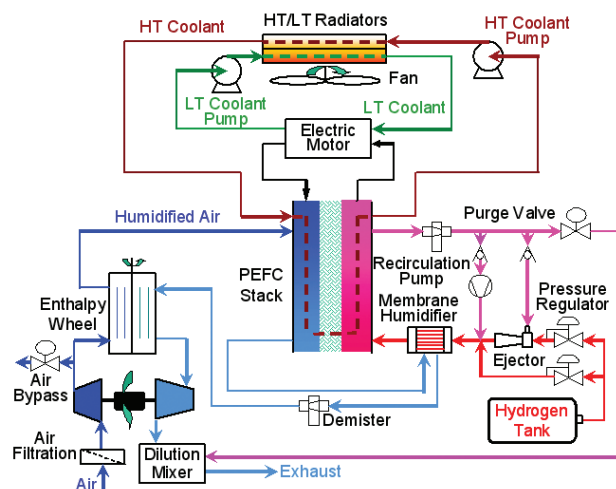


FIGURE 5. Pressurized Automotive Fuel Cell System and Components

three systems with identical layouts, as shown in Figure 5, but different cell voltages at rated power: 0.7 V in S1, 0.65 V in S2, and 0.6 V in S3. In each system, the stack operates at 2.5 bar at rated power, 50% O<sub>2</sub> utilization and 70% H<sub>2</sub> utilization per pass, and has 9.6 cells per inch. The cell MEA consists of anode and cathode catalyst inks deposited onto the GDLs (275- $\mu$ m woven carbon cloths), which are hot-press laminated with the 50  $\mu$ m Nafion<sup>®</sup> membrane. The Pt loading is 0.50 mg/cm<sup>2</sup> on the cathode and 0.25 mg/cm<sup>2</sup> on the anode. The flow channels are fabricated from 2-mm expanded graphite plates and each plate has cooling channels.

As shown in Table 1, our simulations indicate that only S1 meets the 2005 targets of 55% stack and 50% system efficiency at rated power. However, S1 does not satisfy the targets of 1,500 W/L stack power density, 1,500 W/kg stack specific power, or 1 g/kW PGM loading. Conversely, S2 and S3 meet the power density, specific power, and PGM loading targets, but not the stack and system efficiency targets.

None of the systems analyzed achieves the target of 60% efficiency at 25% rated power. The electric motors for the air management system and the radiator fan are the main sources of parasitic power consumption.

Table 1 also shows that all three systems meet the system targets for specific power (500 W/kg) and power density (500 W/L). Since the heat rejection system can be bulky, a study was conducted to evaluate alternatives to the standard automotive radiators (louver fins, 15 fins/inch). We evaluated advanced automotive (louver fins, 25 fins/inch), microchannel (plain fins, 40 fins/inch) and foam (8 wt% Al foam, 40 pores/inch) configurations by considering specific heat transfer, specific pressure drop, and fan power. In terms of the fan power for specified frontal area and heat rejection, the microchannel configuration was judged as the best

TABLE 1. Performance of Fuel Cell System Components

		S1	S2	S3
Cell voltage at rated power	V	0.7	0.65	0.6
<b>PEFC Stack</b>				
Active membrane area	m <sup>2</sup>	19.6	13.6	10.9
Pt loading	g/kW	1.64	1.12	0.90
Current density	A/cm <sup>2</sup>	0.65	1.03	1.40
Power density	mW/cm <sup>2</sup>	458	668	838
Stack specific power	W/kg	1259	1860	2359
Stack power density	W/L	1240	1727	2082
Stack efficiency	%	55.5	51.7	47.6
<b>FCS Parasitic Loads</b>				
PEFC Stack	kWe	89.7	90.6	91.5
CEM motor	kWe	6.1	6.6	7.3
Enthalpy wheel motor	W/e	30	30	30
Radiator fan	kWe	2.7	2.7	2.7
Coolant pump	kWe	0.8	1.0	1.1
H <sub>2</sub> recirculation pump	W/e	252	271	269
FCS efficiency	%	49.5	45.7	41.7
<b>FCS Component Weights</b>				
PEFC stack	kg	72	52	44
Air management system	kg	18	19	21
Fuel management system	kg	7	7	7
Heat rejection system	kg	12	14	17
Water management system	kg	9	10	11
Miscellaneous	kg	12	10	10
Total weight	kg	130	113	110
FCS specific power	W/kg	616	705	725
<b>FCS Component Volumes</b>				
PEFC stack	L	71	49	39
Air management system	L	15	16	18
Fuel management system	L	9	10	11
Heat rejection system	L	35	41	47
Water management system	L	8	9	10
Miscellaneous	L	14	13	12
Total volume	L	152	138	137
FCS power density	W/L	528	581	586

and the foam configuration as the worst performers. Also, the advanced automotive configuration performed better than the standard automotive design.

## Conclusions and Future Directions

- Rapid start of a PEFC stack from subfreezing temperatures unavoidably involves the formation of ice within the porous cathode catalyst and electrode structure. Managing the buildup of ice is the key to obtaining a successful self-start. The stack temperature must be raised above the melting point of ice before the ice can completely cover the cathode catalyst and shut down the electrochemical reaction. Results from our model suggest that for rapid self-start it is desirable to operate the stack near short-circuit conditions.
- Our analyses show that even with no N<sub>2</sub> in the fuel H<sub>2</sub>, nitrogen crossover across the polymer electrolyte membrane may result in the buildup of

$N_2$  concentrations of several percent in the anode inlet gas and about 20% in the anode outlet gas, under the optimum purge conditions. With 0.5%  $N_2$  in the fuel,  $N_2$  may build up to 8% to 18% in the anode inlet and about 40% in the anode outlet (for the cases and parameter values considered in these analyses). The effect of this buildup of  $N_2$  on the overall system efficiency is relatively small, however, typically being less than one percentage point.

- The DOE 2005 targets for fuel cell system specific power, power density, and PGM loading can be satisfied by lowering the cell voltage at rated power and, thus, sacrificing efficiency by a small amount.
- Rejection of low-grade waste heat produced by the stack requires a radiator with a large frontal area and a blower fan that consumes  $>2$  kW. Alternative radiator configurations, such as advanced automotive and microchannel designs, are preferred over the standard automotive radiators.
- Further validate the model on self-start of PEFC stacks from sub-freezing temperatures with data obtained at Argonne.
- Continue collaboration with Honeywell on thermal and water management, if that project is extended.
- Expand work on impurity effects.
- Include long-term degradation effects (durability issues) in systems analysis.
- Continue work on anode gas system.
- Incorporate performance losses due to startup, shutdown, purge, and flooding.
- Participate in the technology validation effort and explore combined heat and power applications of stationary PEFC systems.
- Continue to support DOE/FreedomCAR & Fuel development efforts.

## FY 2006 Publications/Presentations

1. S. Ahmed, R. Ahluwalia, S. H. D. Lee, and S. Lottes, "A Gasoline Fuel Processor Designed to Study Quick-Start Performance," *Journal of Power Sources*, 154, 214-222, 2006.
2. R. K. Ahluwalia, Q. Zhang, D. J. Chmielewski, K. C. Lauzze, and M. A. Inbody, "Performance of CO Preferential Oxidation Reactor with Noble-Metal Catalyst Coated on Ceramic Monolith for On-Board Fuel Processing Applications," *Catalysis Today*, 99, 271-283, 2005.
3. R. K. Ahluwalia, X. Wang, A. Rousseau, and R. Kumar, "Fuel Economy of Hybrid Fuel Cell Vehicles," *Journal of Power Sources*, 152, 233-244, 2005.
4. R. K. Ahluwalia and X. Wang, "Direct Hydrogen Fuel Cell Systems for Hybrid Vehicles," *Journal of Power Sources*, 139, 152-164, 2005.
5. R. K. Ahluwalia and X. Wang, "Rapid Self-Start of Fuel Cells from Subfreezing Temperatures," *2005 Fuel Cell Seminar*, Palm Springs, CA, November 14-18, 2005.
6. R. K. Ahluwalia and X. Wang, "Startup of Fuel Cells from Subfreezing Temperatures," *IEA PEFC Annex XVII Meeting*, Loughborough, U.K., November 30-December 1, 2005. 1.

## References

1. Y. Hishinuma, T. Chikahisa, F. Kagami and T. Ogawa, "The Design and Performance of a PEFC at a Temperature below Freezing," *JSME International J., Series B*, 47, No. 2, 235-241, 2004.
2. C. Mittelsteadt and M. Umbrell, "Gas Permeability in Perfluorinated Sulfonic Acid Polymer Membranes," 207th Electrochemical Society Meeting, Toronto, Canada, May 15-20, 2005.